https://doi.org/10.5194/mr-2025-17
Preprint. Discussion started: 31 December 2025
© Author(s) 2025. CC BY 4.0 License.

Open Access MAGNETIC RESONANCE Discussions

Pulsed Electron Paramagnetic Resonance on two Cu(II)-Cage Compounds With Six, Respectively Eight Copper Ions

Leonardo Passerini[1], Eduard O. Bobylev[2], Felix J. De Zwart[2], Henrik Hintz[3], Adelheid Godt[3], Bas de Bruin[2], Joost Reek[2], Martina Huber[2]

[1]Department of Physics, Leiden University, the Netherlands Huygens-Kamerlingh Onnes Laboratory, Molecular Nano Optics and Spins, Leiden, 2333 CA, the Netherlands.
[2]Van't Hoff institute for molecular sciences, University of Amsterdam, Amsterdam, 1090 GD, the Netherlands.
[3]Department of Chemistry, Bielefeld University, Bielefeld, D-33615, Germany

Correspondence to: Martina Huber (huber@physics.leidenuniv.nl)

Abstract. The copper(II) cages $Pd_{12}Cu_6L^{DMAP}{}_{24}$(**Cu6**) and $Pd_{12}Cu_8L^{Pro}{}_{24}$ (**Cu8**), contain six, resp. eight, Cu(II) ions in a complex constituted by palladium ions and organic ligands in a self-assembled nano-meter sphere. Within the sphere, the Cu(II) ions are expected to form polyhedral-like structures. The parent compounds $Pd_{12}M_6L^{DMAP}{}_{24}$ and $Pd_{12}M_8L^{Pro}{}_{24}$ are of interest because of the possibility of introducing a different metal ions for M, such as Cu(II), in a defined arrangement and for catalytic applications, see (E.O. Bobylev, et al. Chemical Science, (2023), *14*, 11840-11849). For structure information, nano-meter distances where measured between the six, respectively eight Cu(II) ions in **Cu6** and **Cu8**. Distances were measured by pulsed double electron electron resonance (DEER) spectroscopy. While DEER is established for measuring distances between pairs of spins, application to multi-spin systems is less common. Since, so far, no reports of DEER with multi-spin interactions between Cu(II) ions were reported, the copper-cages are an ideal model to study them. For **Cu6** and **Cu8**, DEER shows multi-spin interaction, and the method enabled to establish an octahedral arrangement for the Cu-ions in **Cu6**. For **Cu8**, two distances were observed that are consistent with two structural models proposed for **Cu8**, one of which is a cube of Cu-ions.

https://doi.org/10.5194/mr-2025-17
Preprint. Discussion started: 31 December 2025
© Author(s) 2025. CC BY 4.0 License.

Open Access MAGNETIC RESONANCE Discussions

1 Introduction

Nanometer-distance determination by pulsed EPR methods such as double electron-electron resonance (DEER or PELDOR) has proven its value in many areas of chemistry and biology [12-16]. Much of the applications and theory of interpretation focusses, so far, on two-spin systems, as reviewed in [17, 18]. Multi-spin interactions, where more than two spins interact within a nano-object, have recently come into the focus of research, but so far they are less explored than two-spin interactions. Most of the current multi-spin-interaction investigations were performed on paramagnetic centers with low anisotropy, such as nitroxides [25, 26], and in one case Gd(III) ions [27]. In the present study we turn to multi-spin interactions of paramagnetic centres with larger anisotropy, here, Cu(II) systems (see Fig. 1). In many areas from biology to chemistry, multispin systems, in which more than two

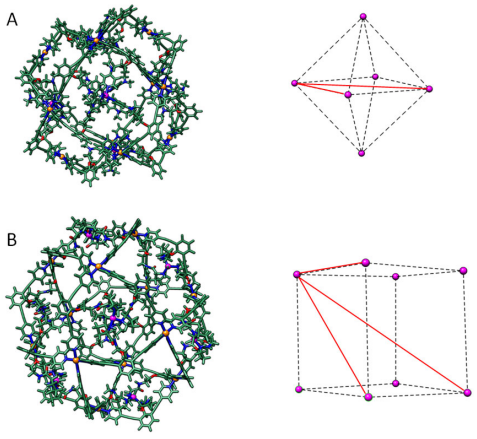

Figure 1. Structures of the Cu(II) cages studied in this work (left), and sketch of the spatial arrangement of the coordinated copper ions (right). A) Cu6. The copper ions are located in the six square windows of the nanosphere, forming an octahedron, giving a total of 2 different distances, highlighted in red. B) Cu8. The copper ions are located in the triangular windows of the nanosphere, forming a cube, giving a total of three different distances. Magenta spheres: copper ions, yellow spheres: palladium ions, green: functional groups coordinating the copper ion, red lines: highlight of the different copper distances inside the cages. For details, see [5].

units interact at nano-meter distances, are of interest. Examples are multimeric protein (sub-) units in biochemistry [1-4] or multiple (transition) metal-ion centers in molecular catalysts [1, 6, 7]. For the latter, there has recently been a surge of interest in radical-based supramolecular systems, owing to their diverse properties and promising applications [8]. The presence of multiple spins within a confined spatial arrangement and a defined geometric structure in such systems gives rise to adjustable spin-spin interactions [9-11]. Moreover, encapsulation of paramagnetic guest molecules creates promising candidates for sensor materials [8-11]. The integration of radicals and metal ions into supramolecular architectures also gives them redox properties for potential catalytic

https://doi.org/10.5194/mr-2025-17
Preprint. Discussion started: 31 December 2025
© Author(s) 2025. CC BY 4.0 License.

Open Access MAGNETIC RESONANCE Discussions

applications [5, 7, 8]. In the past, the analysis of radical-based supramolecular systems predominantly relied on continuous wave electron paramagnetic resonance (EPR) techniques [9-11]. Pulsed EPR adds the possibility of obtaining structural information, and in particular, pulsed dipolar EPR spectroscopy that provides nano-meter distance constraints is promising.

If more than two spins interact in the DEER sensitive distance range, the modulation depth becomes larger than in two-spin systems. For a two-spin system, the modulation depth is given by the inversion efficiency λ, whereas for multispin systems the modulation depth Δ is given by equation:

$$\Delta_N = 1 - (1 - \lambda)^{N-1} \qquad (1)$$

where N is the number of interacting spins [19]. This increase in modulation depth was used as a method for counting monomers in nanoobjects, first by Tsvetkov et al. [20, 21], in oligomers of biological systems [19, 22-24]. Additionally, ghost peaks in the distance distributions can occur. These peaks do not represent actual distances, but derive from sum- and difference-frequencies of the dipolar frequencies measured by DEER [25]. Such ghost peaks can obscure the pair-wise distances and thereby interfere with using DEER distances for structural information. Approaches proposed to identify and suppress ghost peaks are proposed in literature [25-28]. Among those, adjustment of inversion efficiency is the most common method that can be used during data acquisition, by reducing the power of the pump-pulse. Also, see von Hagens et al. [25], power scaling in processing the data is possible. This method is commonly known as "ghost suppression", as it suppresses the ghost distances [25]. On systems containing up to eight nitroxides Valera et al. [27] showed that while power scaling or reduction of the inversion efficiency alone are not enough, a combination of the two still allows for reliable extraction of spin-pair distances, even though the expected relative intensities of the distance peaks were not recovered [27]. Considering metal ions, there is only one study, by Edwards et al. [29], where DEER experiments were performed on a labelled proteorhodopsin hexamer, comparing nitroxide and Gd(III) based spin labels. Multispin effects in the Gd(III) labelled samples were strongly reduced with respect to nitroxides, an effect that was attributed to the naturally low inversion efficiency for Gd(III) [29].

Here we investigate multi-spin interactions in the copper(II) cages Pd12Cu6 ($Pd_{12}Cu_6L^{DMAP}_{24}$)(**Cu6**) and Pd12Cu8 ($Pd_{12}Cu_8L^{Pro}_{24}$) (**Cu8**) (fig.1), with six, respectively eight Cu(II) ions. The synthesis, structural characterization and catalytic interest in these systems were described in [5]. The copper ions in these cages are arranged in approximately octahedral (**Cu6**) or cubic (**Cu8**) shapes (fig. 1). The presence of a relatively large number of Cu(II) ions in a defined arrangement make the cages an ideal system to test multi-spin effects in Cu(II) systems. It has to be noted that the Cu(II)-derivatives of the cage molecules investigated here are not as stable as the term "model compounds" may imply. Prolonged handling at room temperature causes decay, and the Cu(II) centers have a tendency to reduce to Cu(I) making them EPR inactive [5].

In the present study, the application of 9 GHz DEER on the multi-copper cages shown in Fig. 1 is described, revealing multispin interactions, i.e. the interaction of more than two spins. The distances measured agree with those expected for the structures shown in Fig. 1A (**Cu6**) and 1B (**Cu8**).

2 Materials and Methods

2.1 EPR spectroscopy

https://doi.org/10.5194/mr-2025-17
Preprint. Discussion started: 31 December 2025
© Author(s) 2025. CC BY 4.0 License.

Open Access MAGNETIC RESONANCE Discussions

Pulsed EPR measurements were performed at 9 GHz on an Elexsys E680 spectrometer (Bruker) using a 3 mm ER 4118 X-MD-3-W1 split-ring resonator. The cryogenic temperature of 20K was obtained with helium gas in a CF935 (Oxford Instruments) cryostat with an ITC502 temperature controller (Oxford Instruments). Samples were prepared in 3 mm outer-diameter quartz tubes, frozen and stored in liquid nitrogen before insertion into the precooled helium gas-flow cryostat.

The four-pulse DEER [4, 5] sequence $(\pi/2)_1$-τ_1- $(\pi)_1$–$(\tau_1 + t)$-$(\pi)_2$–$(\tau_2$-$t)$-$(\pi)_1$–τ_2-[echo] was employed, where subscripts 1 and 2 indicate events occurring at the observer and pump frequency, respectively. The pump and observer frequencies were separated by 75 MHz. The power of the pump pulse was adjusted to invert the echo maximally. The lengths of the pulses at the observer frequency were 16 and 32 ns for the π /2 and π pulses, respectively. The length of the pump pulse was 16 ns. In the measurements, the τ time was incremented with 8 ns steps starting at τ = 140 ns to suppress nuclear modulation. The slices were added to obtain hyperfine-modulation-free time traces and phase corrected. Regular traces were measured with a total evolution time of 2152 ns. For modulation- depth comparison, a separate experiment with shorter evolution time and a back-to-back measurement of **Cu6**, **Cu8** and **Cu2** was performed.

The DEER data were analyzed using the DeerAnalysis2019 and DeerAnalysis2023 programs [30], which are available from http://www.epr.ethz.ch/ software/index. DeerAnalysis2019 version was used for Tikhonov regularization and Gaussian fitting, while DeerAnalysis2023 was used for DEERNet analysis. Contribution of a known instrumentation artifact at 1940 ns could not be completely eliminated from the real part, therefore all traces were truncated to 1932 ns. Zero time of the traces was 88 ns. After background correction of the data using a three-dimensional background, the distance distribution was determined by Tikhonov regularization, with a regularization parameter of 125. Validation was performed using the validation tool in DeerAnalysis. For **Cu6** the white-noise contribution was varied between 0.02 and 1.5 with 10 steps, and the background start from 372 ns to 1000 ns with 20 steps. For **Cu8** the white-noise contribution was varied between 0.03 and 1.5 with 10 steps, and the background start from 372 ns to 1000 ns with 20 steps. The shaded areas in the distance distribution plots show, for a given distance, the lower and upper error bounds (two times the standard deviation) calculated over all the validation steps.

2.2 Sample Preparation

Cu6 and **Cu8** were synthesized as described in [5]. **Cu2** was synthesized as described in [31]. Samples: **Cu6** and **Cu8**: solvent: 3 : 1 butylnitrile : acetonitrile, copper concentration 0.63 mM (**Cu6**) and 0.83 mM (**Cu8**). **Cu2** solvent: 50% v/v glycerol : water solution, concentration 0.6 mM

3 Results

In this study, DEER data were acquired by 9 GHz EPR spectroscopy on the **Cu8** and **Cu6** cages. A two-copper complex (**Cu2**), structure see Fig. SI2, was used as reference [31]. In the following, we present the outcome of the characterization.

https://doi.org/10.5194/mr-2025-17
Preprint. Discussion started: 31 December 2025
© Author(s) 2025. CC BY 4.0 License.

Open Access MAGNETIC RESONANCE Discussions

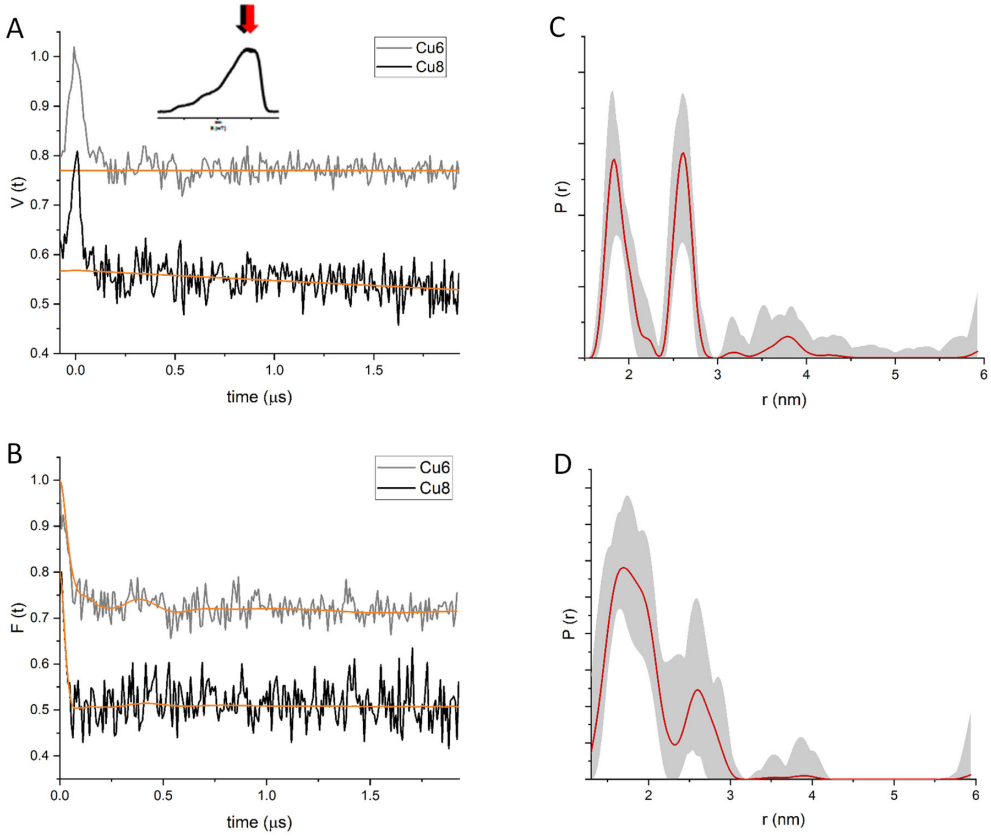

Figure 2. Results of DEER experiments of the Cu6 and Cu8 cages. A) Raw DEER traces. Gray: Cu6, black: Cu8. Orange: background. B) Background subtracted DEER traces with fits (orange). Gray: Cu6 trace, black: Cu8. C) Distance distribution obtained for Cu6 (red). D) Distance distribution obtained for Cu8 (red). Maximum echo intensity (A,B) is normalized to unity, Cu8 traces have been downshifted for better visibility. Shaded area in C) and D): standard deviation of each point in the distance distribution, by validation DEERAnalysis. Inset: field-swept-echo EPR spectrum of Cu6. Arrows: position of pump (red) and observer (black) frequency. V(t) : primary measured data, normalized to maximum intensity. F(t) : form factor obtained after background subtraction. For details and experimental parameters, see text.

The DEER traces obtained for **Cu8** and **Cu6** are shown in Fig. 2A. The length of the traces is 2 µs, a length that is similar to the DEER evolution time obtained in similar experiments on Cu(II)-pairs in the literature [32-34]. The traces of **Cu8** and **Cu6** are clearly different from one another. Both show an initial fast decay, which suggests the presence of short distances. In **Cu6**, there is a clear modulation maximum around 450 ns, while for **Cu8** there are

https://doi.org/10.5194/mr-2025-17
Preprint. Discussion started: 31 December 2025
© Author(s) 2025. CC BY 4.0 License.

Open Access MAGNETIC RESONANCE Discussions

no clear oscillations. The difference between the two traces is even more evident in Fig. 2B, where the traces are shown after background subtraction.

In Fig. 2C and 2D the distance distributions are shown. They are obtained considering only spin-pair contributions. A detailed analysis of the DEER data using DeerNet, validation and ghost suppression is described in the SI. For **Cu6** (Fig. 2C) two distinct distance peaks are observed, one is centered around 1.8 nm , and a second peak with approximately the same intensity is centered around 2.6 nm (see Table 1). A peak with a small population around 3.6 nm is seen, but validation shows that this peak is not reliable. The distance distribution of the **Cu8** cage (Fig. 2D) also has two distance peaks, one at 1.8 nm that is broader than the one in **Cu6**, and has a shoulder around 2 nm. The second distance peak in **Cu8** is located at 2.8 nm, its intensity is smaller than the one at 1.8 nm. A peak with a small population around 3.8 nm is also seen in **Cu8**, yet it is not reliable, see validation. All relevant distances

Table 1. DEER distances, modulation depth and model-derived distances for Cu6 and Cu8. <r>: center of peak. Δ: measured modulation depth of the background-subtracted DEER traces. The expected intensity ratio is valid for both model 1 (M1) and model 2 (M2). DEER results are processed by Tikhonov regularization. The deviations of the model from ideal geometrical bodies are determined from the differences in Cu-Cu distances of Cu-pairs that would be equivalent in the ideal body. Modulation depth of Cu2 λ = 13 ±1%.

are given in Table 1. The distance peaks obtained for **Cu6** are narrower than the ones obtained for **Cu8**, in the latter sample, the peak shape is irregular, which could hint at several distances contributing.

Cu6 distances from DEER	Cu6 M1	Cu6 M2	expected intensity ratio Cu6	Cu6 Δ %	Cu8 distances from DEER	Cu8 M1	Cu8 M2	expected intensity ratio Cu8	Cu8 Δ %
<r> (nm)	r (nm)	r (nm)			<r> (nm)	r (nm)	r (nm)		
1.8	1.8 ± 0.3	1.7 ± 0.3	4	23 ± 2	1.8	2.0 ± 0.1	2.2 ± 0.6	3	22 ± 2
2.6	2.6 ± 0.3	2.7 ± 0.2	1		2.6	2.8 ± 0.1	3.1 ± 0.6	3	
						3.5± 0.14	3.8 ± 0.2	1	

In general, the width of the distance peaks is maximally 0.2 nm full width at half maximum (FWHM), in line with spin pairs in other rigid copper systems reported in the literature [31].

https://doi.org/10.5194/mr-2025-17
Preprint. Discussion started: 31 December 2025
© Author(s) 2025. CC BY 4.0 License.

Open Access MAGNETIC RESONANCE Discussions

Since modulation depth strongly depends on experimental conditions, **Cu2** [31] was used as a reference compound. It contains two Cu(II) ions at a distance of 3.3 nm. The DEER properties of this reference sample agree with those measured before [31]. In Fig. 3, the DEER trace of **Cu2** (green trace) is shown alongside the DEER traces of **Cu6** and **Cu8**. The modulation depth is 23 % for **Cu6**, 22 % for **Cu8**, and 13 % for **Cu2**. Higher modulation depth is associated with multispin effects, revealing that the **Cu6** and **Cu8** DEER traces show interactions between more than two Cu(II) ions. Quantitatively, equation 1 gives the relation between the number of interacting electron spins N and the modulation depth. For the cages, this relation shows interaction of approximately three spins, a number we will discuss in detail below.

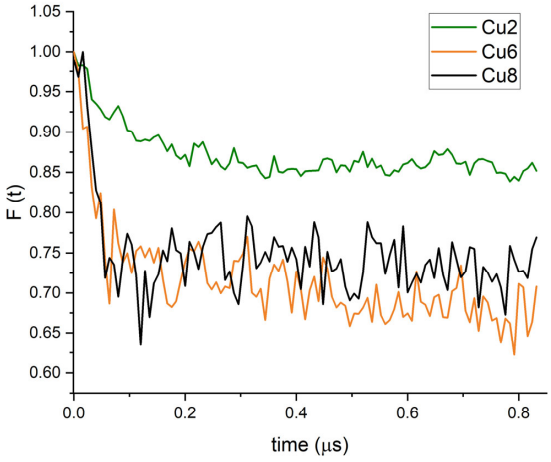

Figure 3. Comparison of the modulation depth of Cu6 and Cu8 with that of Cu2. DEER traces (background subtracted) obtained for Cu6, Cu8 and Cu2, containing two Cu(II) ions at a distance of 3.3 nm. Green trace: Cu2, orange: Cu6, black: Cu8. Modulation depth of Cu2 λ = 13%. In all traces maximum DEER-trace intensity is normalized to unity. For better S/N ratio, traces of Cu6 and Cu8 have shorter evolution time than in Fig. 2. For details and experimental parameters, see text.

Interaction of multiple spins with distances in the DEER sensitive range not only affects the modulation depth, but can also give rise to sum- and difference-frequencies that can manifest themselves as extra peaks in the distance distribution, so called ghost peaks. In Fig. 4, the effects of the application of the ghost suppression tool in DeerAnalysis, see Materials and methods, are shown for three interacting spins. Similar effects are seen for higher numbers of spins, see Fig. SI5 and SI6 in the SI. The changes in the distance distribution upon ghost suppression (Fig. 4) are small, and none of the peaks are completely suppressed, showing that they are not ghost peaks. For **Cu6**, the longer distance peak (around 3.8 nm) shows the largest difference, but this distance was already considered non reliable after validation. For **Cu8**, small differences are also observed for the small feature between

https://doi.org/10.5194/mr-2025-17
Preprint. Discussion started: 31 December 2025
© Author(s) 2025. CC BY 4.0 License.

Open Access MAGNETIC RESONANCE Discussions

3.5 and 4 nm. In the latter case, it appears that the peak shifts to a different distance, suggesting even more care when interpreting this distance.

Expected distances for the Cu cages

From quantum-mechanical calculations, model structures for **Cu6** and **Cu8** were obtained [5]. For **Cu6** and **Cu8**, two possible structures were found, which differ in the location of the Cu ions and thereby the Cu-Cu distances. In Fig. SI1, both models are shown. As described in detail in Bobylev *et al.* [5], for **Cu6**, model 1, the Cu ions are located in the six square windows of the nanosphere, creating a shape close to an octahedron, see Fig. 1A, whereas in model 2, four copper ions are located below a palladium center and two in the square windows of the nanosphere (see SI for comparison of models 1 and 2 for **Cu6** and **Cu8** respectively). For **Cu8,** model 1, with the Cu-ions in the triangular windows, the copper ions are located at the corners of a cube, see Fig. 1B and SI1, while in model

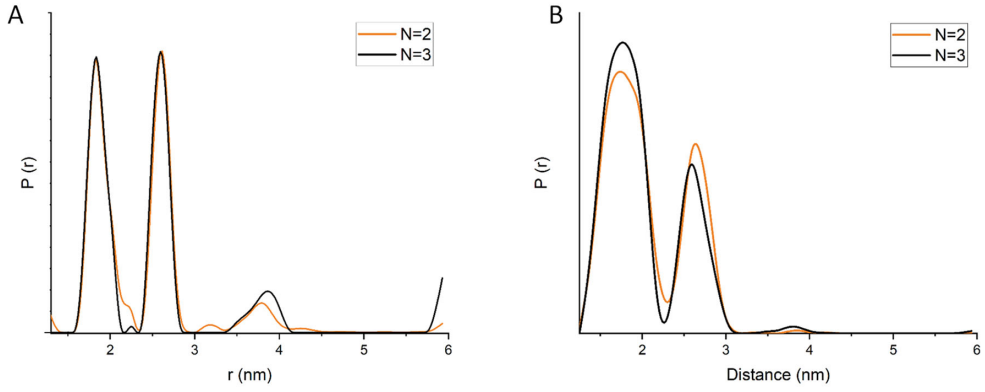

Figure 4. Effect of ghost suppression on distance distribution for three (N = 3) spins, compared with distance distribution for two (N = 2) spins. A) Effect of ghost suppression on Cu6. B) Cu8. Orange: distance distribution obtained without ghost suppression N = 2, black: distance distribution obtained with ghost suppression for N=3 spins. The areas below the P(r) curves were normalized to unity.

2, six copper-ions are in the square windows and two in the triangular windows, forming a distorted cube (see Fig. SI1).

To derive expected Cu-Cu distances from the models, all pairwise Cu-Cu distances in the model were measured, and then grouped into distances that are equivalent in an ideal octahedron, or a cube, respectively. For each of these groups, in table 1, the average distance and the maximum spread is given. Therefore, a large spread shows a strong deviation of the model from the ideal body. For **Cu6**, the average Cu-Cu distances of model 1 and model 2 are slightly different from each other, see table 1. However, they overlap within the spread of the distances in each model, showing that deciding on a model is difficult on the basis of the Cu-Cu distances alone. A similar situation pertains for **Cu8**, and for this cage the spread, especially for model 2, is even larger than for **Cu6**.

Equivalent distances in the models

https://doi.org/10.5194/mr-2025-17
Preprint. Discussion started: 31 December 2025
© Author(s) 2025. CC BY 4.0 License.

Open Access MAGNETIC RESONANCE Discussions

In principle, each pair of Cu ions within the distance range of the DEER experiment is expected to contribute to the distance distribution. Considering the geometric structure of the cages according to model 1 (Fig. 1), each Cu(II) ion has multiple neighbors with a distance within the DEER range. For **Cu6**, model 1, each Cu(II) ion has four neighbors at a distance of 1.8 nm, and one at a distance of 2.6 nm, so the expected intensity ratio of the two respective distance peaks should be 4:1. For **Cu8,** model 1, each Cu(II) ion is expected to have three neighbors at 2 nm, three at 2.8 nm and one at 3.4 nm, so the expected ratio of the distance peaks is 3:3:1. For model 2, the same intensity ratios are expected as for model 2, as long as it can be considered an almost ideal geometrical body.

Comparison of model distances with DEER distances

For **Cu6** the distances found by DEER agree slightly better with the average distances in model 1, in agreement with conclusions drawn from other experimental evidence in Bobylev *et al.* [5]. For **Cu8**, Model 1 predicts two distances (2.0 and 2.8 nm) that are close to the experimental ones and a long distance (3.4 nm) that is not observed. The latter distance may be difficult to observe in the DEER experiments, see discussion. For **Cu8**, the DEER distances are closer to the average of the Cu-Cu distances predicted by model 1, however the spread of distances in model 2 is so large that an assignment is not possible.

4 Discussion

Here, we demonstrate DEER on multi-spin systems with Cu(II) ions. We show that reliable distances can be determined and that ghost peaks do not form an obstacle. Two Cu-cages were investigated, comprising six (**Cu6**) and eight (**Cu8**) Cu(II) ions, respectively, in cage-like arrangements (see Fig. 1). The structure of the cages was previously determined by a variety of techniques, as described in [5], where also the synthesis and spectroscopic characterization can be found. Here we describe the detailed investigation of these copper cages by DEER spectroscopy, to determine the distances between the Cu(II) ions and the impact of multispin interaction.

For both **Cu6** and **Cu8,** two models were proposed that differ in the location of the copper ions within the cage. For **Cu6** the measured distances are in better agreement with the average distances predicted from model 1, see table 1. That assignment agrees with [5] and firmly places the copper ions in the square windows of the Pd-ions, as shown in Fig. 1B. Whereas the distances observed in the DEER experiment agree well with those expected (table 1), the intensity of the DEER distance peaks deviate: The relative intensities of the distance peaks is 1:1, while 4:1 is expected (see table 1). Possible reasons for the too low intensity of the shorter distance peak (1.8 nm), amongst which orientation selection, are discussed in the SI.

For **Cu8**, models 1 and 2 predict three distances, of which the shorter two agree with the experimentally observed ones, whereas the longest distance (3.4 nm, model 1, 3.8 nm, model 2) is not observed experimentally (table 1). Several factors can contribute to the absence of the longest distance. The contribution of the longest distance to the distance distribution should be smaller, since the longest distance in the cube represents only a single Cu-Cu pair. Nevertheless, at the expected ratio of 3:3:1 (table 1) it should still be seen. Another contribution could be the uncertainty in the background correction in combination with the relatively short evolution time, and perhaps, that there is a large spread in distances, leading to a broad distance distribution that would make the peak difficult to

https://doi.org/10.5194/mr-2025-17
Preprint. Discussion started: 31 December 2025
© Author(s) 2025. CC BY 4.0 License.

Open Access MAGNETIC RESONANCE Discussions

detect. In contrast to **Cu6**, the model for **Cu8** deviates strongly from the ideal body, as seen particularly for model 2. In [5], it was suggested that the copper ligands, e.g. the pyrrolidine ligands [5], could have different orientations, leading to a spread in copper positions and thereby broader distance distributions, or a coexistence of the two **Cu8** model structures. Both possibilities could also lead to the larger width and more asymmetric shape of the distance peaks in **Cu8** compared to **Cu6**. Also, the signal-to-noise ratio of the **Cu8**-DEER traces is lower than for **Cu6**, which also derives from the shorter T_2 relaxation time of **Cu8** compared to **Cu6** (see SI).

Summarizing, all peaks observed in the distance distributions in **Cu6** and **Cu8** are accounted for by the expected pairwise distances. The distances found for **Cu6** and **Cu8** are reliable, since ghost suppression does not abolish any of the distance peaks, revealing that all distance peaks of **Cu6** and **Cu8** are real. Additionally, as all peaks observed correspond to distances expected for the Cu-cages, full suppression of individual peaks is not likely.

The larger modulation depth of **Cu6** and **Cu8** compared to the reference compound (see results, Fig. 3) clearly shows that more than two spins interact, however, the number of interacting spins is lower than six (**Cu6**) resp. eight (**Cu8**), and several sources can contribute to the lower number. First, there is the uncertainty in the number of interacting spins that derives from the signal-to-noise ratio of the DEER data (Fig. 3) of both, the Cu-cages, and the reference compound (**Cu2**), an effect that is compounded by the short phase memory time, T_m of the Cu-cages. Other effects, such as orientation selection and chemical factors, for example reduction of some of the Cu(II) centers in the cages, are difficult to quantify, but they would all lower the number of interacting spins, as described in the SI. Experimentally, some of these factors could be tackled, however, given the fragility of these samples this was not feasible (for details, see SI). Consequently, both Cu-cages show clearly that the interaction is between more than a pair of spins, yet, the factors described result in a number of interacting spins that is significantly lower than expected.

Unwanted multispin effects, such as ghost peaks (Fig. 4 and Fig. SI5 and SI6), are weak in comparison with theoretical studies of multispin effects [25-27] and experimental results [22, 27, 29, 35-38, 39] described in the literature. An obvious difference is that most of these systems are nitroxide based. Nitroxides have a smaller spectral anisotropy than the Cu(II) centers investigated here, resulting in a higher pump-pulse-inversion efficiency λ compared to Cu(II). A clear indication of the small λ of the Cu(II) systems investigated here is the modulation depth Δ of only 13 % for **Cu2**, a two-Cu(II) system with $\lambda = \Delta$, whereas for two-spin interactions in nitroxides modulation depths of around 50 % are standard at 9.5 GHz DEER [17]. Low pump-pulse-inversion efficiency also translates to low multispin excitation and thereby low ghost-peak intensities, as Edwards et al. have shown [29]. In the latter work, nitroxides had stronger ghost-peak contributions than Gd(III) labels, in agreement with the larger spectral anisotropy of Gd(III) with respect to nitroxides [29]. Evidently, this is also the case for the copper cages. Further reduction of multispin effects could have been obtained by lowering the inversion efficiency and power scaling [25-27], however, in view of the already small effects we did not try these.

The relative intensities of the distance peaks differ from those expected from the model, see above. One explanation could be that the intensities are affected by ghost-peak effects. For example, Valera *et al.* [27] found that not in all cases ghost-peak suppression recovers the expected distance-peak intensities. Also, orientation selection could play a role, see SI, however, no quantitative estimate can be given at this point.

In conclusion, the two copper cages **Cu6** and **Cu8**, show that multispin effects can also be tackled in Cu(II)-based systems and that DEER is an excellent tool to obtain structure information in multi-copper systems. This extends

https://doi.org/10.5194/mr-2025-17
Preprint. Discussion started: 31 December 2025
© Author(s) 2025. CC BY 4.0 License.

Open Access MAGNETIC RESONANCE Discussions

the reach of DEER for multispin systems, whether biological or chemical, be it for catalysis systems or those of interest for material sciences.

References

[1] M.J. Wiester, P.A. Ulmann, C.A. Mirkin, Enzyme mimics based upon supramolecular coordination chemistry, Angew Chem Int Ed Engl 50(1) (2011) 114-37.
[2] T. Brugnari, D.M. Braga, C.S.A. dos Santos, B.H.C. Torres, T.A. Modkovski, C.W.I. Haminiuk, G.M. Maciel, Laccases as green and versatile biocatalysts: from lab to enzyme market—an overview, Bioresources and Bioprocessing 8(1) (2021).
[3] R. Guo, J. Gu, S. Zong, M. Wu, M. Yang, Structure and mechanism of mitochondrial electron transport chain, Biomed J 41(1) (2018) 9-20.
[4] P. Brzezinski, A. Moe, P. Adelroth, Structure and Mechanism of Respiratory III-IV Supercomplexes in Bioenergetic Membranes, Chem Rev 121(15) (2021) 9644-9673.
[5] E.O. Bobylev, L. Passerini, F.J. de Zwart, D.A. Poole, S. Mathew, M. Huber, B. de Bruin, J.N.H. Reek, Pd12MnL24 (for n = 6, 8, 12) nanospheres by post-assembly modification of Pd12L24 spheres, Chemical Science 14 (2023) 11840-11849.
[6] M. Ruben, J.M. Lehn, P. Muller, Addressing metal centres in supramolecular assemblies, Chem Soc Rev 35(11) (2006) 1056-67.
[7] L. Chen, Z. Guo, X.G. Wei, C. Gallenkamp, J. Bonin, E. Anxolabehere-Mallart, K.C. Lau, T.C. Lau, M. Robert, Molecular Catalysis of the Electrochemical and Photochemical Reduction of CO2 with Earth-Abundant Metal Complexes. Selective Production of CO vs HCOOH by Switching of the Metal Center, J Am Chem Soc 137(34) (2015) 10918-21.
[8] B. Huang, L. Mao, X. Shi, H.B. Yang, Recent advances and perspectives on supramolecular radical cages, Chem Sci 12(41) (2021) 13648-13663.
[9] Y. Ozaki, M. Kawano, M. Fujita, Engineering noncovalent spin-spin interactions in an organic-pillared spin cage, Chem Commun (Camb) (28) (2009) 4245-7.
[10] K. Nakabayashi, Y. Ozaki, M. Kawano, M. Fujita, A self-assembled spin cage, Angew Chem Int Ed Engl 47(11) (2008) 2046-8.
[11] W.L. Jiang, Z. Peng, B. Huang, X.L. Zhao, D. Sun, X. Shi, H.B. Yang, TEMPO Radical-Functionalized Supramolecular Coordination Complexes with Controllable Spin-Spin Interactions, J Am Chem Soc 143(1) (2021) 433-441.
[12] S.A.D. K. M. SALIKHOV, AND A. M. RAITSIMRING, The Theory of Electron Spin-Echo Signal Decay Resulting from Dipole-Dipole Interactions between Paramagnetic Centers in Solids, jOURNAL OF MAGNETIC RESONANCE 42 (1981) 255 - 276.
[13] M. Pannier, S. Veit, A. Godt, G. Jeschke, H.W. Spiess, Dead-time free measurement of dipole-dipole interactions between electron spins. 2000, J Magn Reson 213(2) (2011) 316-25.
[14] F.D. Breitgoff, K. Keller, M. Qi, D. Klose, M. Yulikov, A. Godt, G. Jeschke, UWB DEER and RIDME distance measurements in Cu(II)-Cu(II) spin pairs, J Magn Reson 308 (2019) 106560.
[15] M.U. Irene M. C. van Amsterdam, Gerard W. Canters, and Martina Huber, Measurement of a Cu-Cu Distance of 26 A by a Pulsed EPR Method, Angew. Chem. Int. Ed 42(1) (2003) 62-64.
[16] M.M. Roessler, M.S. King, A.J. Robinson, F.A. Armstrong, J. Harmer, J. Hirst, Direct assignment of EPR spectra to structurally defined iron-sulfur clusters in complex I by double electron-electron resonance, Proc Natl Acad Sci U S A 107(5) (2010) 1930-5.
[17] G. Jeschke, DEER distance measurements on proteins, Annu Rev Phys Chem 63 (2012) 419-46.
[18] O. Schiemann, C.A. Heubach, D. Abdullin, K. Ackermann, M. Azarkh, E.G. Bagryanskaya, M. Drescher, B. Endeward, J.H. Freed, L. Galazzo, D. Goldfarb, T. Hett, L. Esteban Hofer, L. Fabregas Ibanez, E.J. Hustedt, S. Kucher, I. Kuprov, J.E. Lovett, A. Meyer, S. Ruthstein, S. Saxena, S. Stoll, C.R. Timmel, M. Di Valentin, H.S. McHaourab, T.F. Prisner, B.E. Bode, E. Bordignon, M. Bennati, G. Jeschke, Benchmark Test and Guidelines for DEER/PELDOR Experiments on Nitroxide-Labeled Biomolecules, J Am Chem Soc 143(43) (2021) 17875-17890.

https://doi.org/10.5194/mr-2025-17
Preprint. Discussion started: 31 December 2025
© Author(s) 2025. CC BY 4.0 License.

Open Access MAGNETIC RESONANCE Discussions

[19] D.M. Bela E. Bode , Jorn Plackmeyer , Gerd Durner, Thomas F. Prisner, Olav Schiemann, Counting the monomers in nanometer-sized oligomers by pulsed electron-electron double resonance, JACS 129 (2007) 6736-6745.
[20] A.D.Milov, Yu.D.Tsvetkov, F.Formaggio, M.Crisma, C.Toniolo, a. J.Raap, The Secondary Structure of a Membrane-Modifying Peptide in a Supramolecular Assembly Studied by PELDOR and CW-ESR Spectroscopies, J. Am. Chem. Soc. 123 (2000) 3784-3789.
[21] A. D. Milov, Yu. D. Tsvetkov, a.J. Raap, Aggregation of Trichogin Analogs in Weakly Polar Solvents: PELDOR and ESR Studies, Appi. Magn. Reson 19 (1998) 215-226.
[22] M.J. Junk, H.W. Spiess, D. Hinderberger, DEER in biological multispin-systems: a case study on the fatty acid binding to human serum albumin, J Magn Reson 210(2) (2011) 210-7.
[23] E.R. Georgieva, P.P. Borbat, H.D. Norman, J.H. Freed, Mechanism of influenza A M2 transmembrane domain assembly in lipid membranes, Sci Rep 5 (2015) 11757.
[24] P.S. Kerry, H.L. Turkington, K. Ackermann, S.A. Jameison, B.E. Bode, Analysis of influenza A virus NS1 dimer interfaces in solution by pulse EPR distance measurements, J Phys Chem B 118(37) (2014) 10882-8.
[25] T. von Hagens, Y. Polyhach, M. Sajid, A. Godt, G. Jeschke, Suppression of ghost distances in multiple-spin double electron-electron resonance, Phys Chem Chem Phys 15(16) (2013) 5854-66.
[26] M.S. Gunnar Jeschke, Miriam Schulteb and Adelheid Godt, Three-spin correlations in double electron–electron resonance, Phys Chem Chem Phys 11(31) (2009) 6580-6591.
[27] K.A. Silvia Valera, Christos Pilotas, Hexian Huang, James H. Naismith, Bela E. Bode, Accurate Extraction of Nanometer Distances in Multimers by Pulse EPR, ChemPubSoc Europe 22 4700 - 4703.
[28] K. Ackermann, B.E. Bode, Pulse EPR distance measurements to study multimers and multimerisation, Molecular Physics 116(12) (2018) 1513-1521.
[29] D.T. Edwards, T. Huber, S. Hussain, K.M. Stone, M. Kinnebrew, I. Kaminker, E. Matalon, M.S. Sherwin, D. Goldfarb, S. Han, Determining the oligomeric structure of proteorhodopsin by Gd3+ -based pulsed dipolar spectroscopy of multiple distances, Structure 22(11) (2014) 1677-86.
[30] V.C. G. Jeschke, P. Ionita, A. Godt, H. Zimmermann, J. Banham, C. R. Timmel, D. Hilger, and H. Jung, DeerAnalysis2006 - a Comprehensive Software Package for Analyzing Pulsed ELDOR Data, Applied Magnetic Resonance 30 (2006) 473 - 498.
[31] K. Keller, I. Ritsch, H. Hintz, M. Hülsmann, M. Qi, F.D. Breitgoff, D. Klose, Y. Polyhach, M. Yulikov, A. Godt, G. Jeschke, Accessing distributions of exchange and dipolar couplings in stiff molecular rulers with Cu(II) centres, Phys Chem Chem Phys 22(38) (2020) 21707-21730.
[32] S. Ghosh, M.J. Lawless, H.J. Brubaker, K. Singewald, M.R. Kurpiewski, L. Jen-Jacobson, S. Saxena, Cu2+-based distance measurements by pulsed EPR provide distance constraints for DNA backbone conformations in solution, Nucleic Acids Res 48(9) (2020) e49.
[33] D.M. Engelhard, A. Meyer, A. Berndhauser, O. Schiemann, G.H. Clever, Di-copper(ii) DNA G-quadruplexes as EPR distance rulers, Chem Commun (Camb) 54(54) (2018) 7455-7458.
[34] J.E. Lovett, A.M. Bowen, C.R. Timmel, M.W. Jones, J.R. Dilworth, D. Caprotti, S.G. Bell, L.L. Wong, J. Harmer, Structural information from orientationally selective DEER spectroscopy, Phys Chem Chem Phys 11(31) (2009) 6840-8.
[35] A. Meyer, J.J. Jassoy, S. Spicher, A. Berndhäuser, O. Schiemann, Performance of PELDOR, RIDME, SIFTER, and DQC in measuring distances in trityl based bi- and triradicals: exchange coupling, pseudosecular coupling and multi-spin effects, Physical Chemistry Chemical Physics 20(20) (2018) 13858-13869.
[36] K. Ackermann, C. Pliotas, S. Valera, J.H. Naismith, B.E. Bode, Sparse Labeling PELDOR Spectroscopy on Multimeric Mechanosensitive Membrane Channels, Biophysical Journal 113(9) (2017) 1968-1978.
[37] A. Meyer, D. Abdullin, G. Schnakenburg, O. Schiemann, Single and double nitroxide labeled bis(terpyridine)-copper(II): influence of orientation selectivity and multispin effects on PELDOR and RIDME, Phys Chem Chem Phys 18(13) (2016) 9262-71.
[38] L. Fabregas-Ibanez, V. Mertens, I. Ritsch, T. von Hagens, S. Stoll, G. Jeschke, Dipolar pathways in multi-spin and multi-dimensional dipolar EPR spectroscopy, Phys Chem Chem Phys 24(37) (2022) 22645-22660.
[39] A. Giannoulis, R. Ward, E. Branigan, J.H. Naismith, B.E. Bode, PELDOR in rotationally symmetric homo-oligomers, Mol Phys 111(18-19) (2013) 2845-2854.